Piezoelectrically induced resistance modulations in $La_{0.7}Sr_{0.3}MnO_3/Pb(Zr,Ti)O_3$ field effect devices

C. Thiele,[a] K. Dörr, and L. Schultz
IFW Dresden, Institute for Metallic Materials, Helmholtzstraße 20, 01069 Dresden, Germany

E. Beyreuther
Institute of Applied Photophysics, Technische Universität Dresden, 01062 Dresden, Germany

W.-M. Lin
Institute for Solid State Electronics, Technische Universität Dresden, 01062 Dresden, Germany

(Received 28 February 2005; accepted 26 August 2005; published online 13 October 2005)

Epitaxial ferroelectric-ferromagnetic field effect devices of $PbZr_{0.52}Ti_{0.48}O_3/La_{0.7}Sr_{0.3}MnO_3$ (PZT/LSMO) with narrow manganite channels ($\leqslant 7$ nm) show butterflylike hysteretic resistance modulations (ΔR) which are commensurate with strain variation from inverse piezoelectric effect of PZT. Based on the type of observed resistance hysteresis loops, contributions from electric field effect and strain effect have been distinguished for devices with varied channel thickness. The strain-induced ΔR decreases with increasing channel thickness. The ΔR from field effect is low in the LSMO channels with 30% Sr doping. © *2005 American Institute of Physics*.
[DOI: 10.1063/1.2108129]

A ferroelectric gate may provide a memory function to the well-known field effect transistor (FET). Therefore, all-oxide structures with a ferroelectric $Pb(Zr,Ti)O_3$ (PZT) gate layer and various oxide channels ($La_{0.7}Ca_{0.3}MnO_3$, $Bi_2Sr_2CuO_6$, and doped $SrTiO_3$) have been investigated.[1–3] Ferromagnetic manganites $R_{1-x}A_xMnO_3$ (R=La, Bi, or rare-earth element; A=nontrivalent doping element) have been introduced as channel materials in such ferroelectric FETs,[1,4] after an earlier investigation demonstrated the bare field effect in manganite films using a dielectric gate.[5] Recent investigations have shown reproducible resistance hysteresis in few nanometer wide manganite channels controlled by the electrical polarization in an adjacent PZT layer.[6–8] Remanent resistance changes reach up to 28% at 300 K.[6] Thus, manganites might not be able to compete with other oxide channel materials regarding the magnitude of the field effect; instead, they are challenging for the control of magnetism by electric field and for the impact of charge-density modulation on their complex phase diagrams in a more fundamental way.

Note, however, that PZT is a ferroelectric with a strong piezoelectric response. Many transition-metal oxides show a strong sensitivity of electronic properties to distortions of the crystal lattice. Therefore, heteroepitaxial growth of bilayer films of the respective oxide and, e.g., PZT opens a perspective towards strain control of electronic properties, as was suggested for manganites by Tabata and Kawai.[4] Clamping of epitaxial film structures by the substrate has been a strong hindrance for this approach so far. Instead, a piezoelectric substrate ($BaTiO_3$) allowed the observation of a 12% change of resistance in $La_{0.5}Sr_{0.5}MnO_3$ at 300 K.[9] However, in this and other experiments, the resistance changes induced by lattice strain and electric field effects have not been distinguished.

In the present work, the shape of resistance hysteresis loops is utilized to distinguish the influences from field effect and piezoelectric effect, since both effects differ regarding the type of hysteresis loop. We have investigated the resistance modulations in a common $La_{0.7}Sr_{0.3}MnO_3/PbZr_{0.52}Ti_{0.48}O_3$ field effect device structure. For devices with narrow (<7 nm) channels, the measured hysteretical resistance loops clearly agree with the loops expected for the in-plane strain from the inverse piezoelectric effect of the PZT layer. The piezoelectric effect dominates over the field effect in the present devices because the latter is very small in $La_{0.7}Sr_{0.3}MnO_3$.

Thin epitaxial $La_{0.7}Sr_{0.3}MnO_3$ (LSMO)/$PbZr_{0.52}Ti_{0.48}O_3$ bilayer films have been deposited on $SrTiO_3$(100) (STO) single-crystal substrates by pulsed laser deposition (PLD) in off-axis geometry.[10] The stoichiometric targets were ablated by a KrF excimer laser (wavelength of 248 nm and pulse energy of 530 mJ). The LSMO films were grown on STO substrates at a temperature of T=820 °C in an oxygen pressure of $p(O_2)$=0.45 mbar and with a pulse repetition rate of f=3 Hz, whereas the PZT films were grown on top of the LSMO layers at 650 °C, $p(O_2)$=0.1 mbar, and f=15 Hz. Appropriate shadow masks positioned on the substrate surface were used to obtain well-defined structures. Devices with varying LSMO channel thickness and 530-nm-thick PZT films have been prepared with growth rates of the order of ~0.1 Å/pulse. The films were cooled down to room temperature in $p(O_2)$=600 mbar. Platinum contacts for electric measurements were laser deposited in on-axis geometry at room temperature at p=0.01 mbar. The film thickness d was measured with an accuracy of 1 nm with a profilometer (DEKTAK) at the structures obtained by the shadow masks. Ferroelectric polarization loops $P(E)$ at f=1.6 Hz in dependence on electric field E were obtained using a standard ferroelectric tester unit in the virtual ground mode. Measurements of the LSMO channel conductance under applied gate voltage have been carried out in the geometry shown in Fig. 1. The 300-μm-wide LSMO channel is covered with PZT dots of 1000 μm diameter. The PZT top surface is electrically contacted via a platinum dot of 500 μm diameter and four platinum dots on the LSMO channel allow four-probe

[a]Electronic mail: c.thiele@ifw-dresden.de

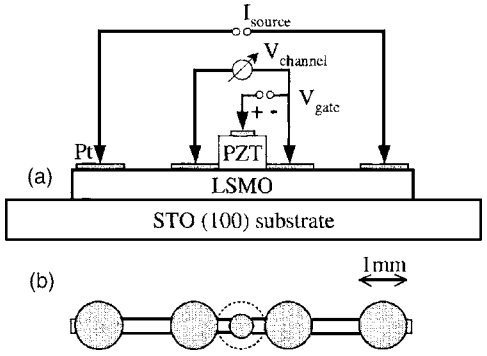

FIG. 1. Schematic lateral structure of the device: (a) cross section and (b) top view.

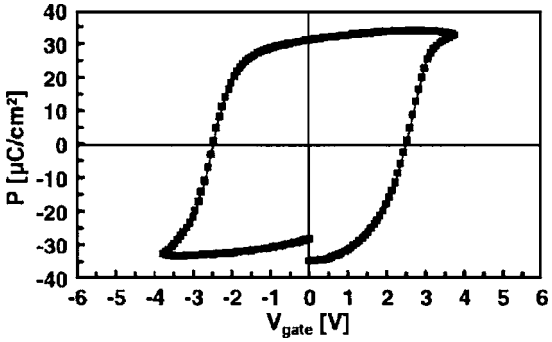

FIG. 3. Polarization in dependence on the applied electrical voltage of a Pt/PZT (530 nm)/LSMO/STO device. Loop centering and lack of loop closure result from the measurement method (RT66A).

resistance measurements. In order to detect the effects of the ferro- and piezoelectric gates onto the LSMO channel, a gate voltage V_{gate} has been applied to the Pt top electrode on the PZT layer. A 3 s time delay between the change of V_{gate} and the channel resistance measurement has been applied in order to allow any switching transients to die down. In this geometry, it is possible to affect approximately half of the channel's length between the voltage ($V_{channel}$) electrodes with the piezoelectric layer. PZT leakage currents had maximum values of a few nanoamperes (compared to source currents of ~ 100 μA) at the respective maximum gate voltages $\pm V_{gate}$ and have been registered during the measurement for each value of V_{gate}. Thus, the resistance measurements could be corrected taking into account the small gate leakage currents.

Both LSMO and PZT films are epitaxially grown in (001) orientation as checked by x-ray analysis.[11] The channel thickness was varied from 5 to 200 nm. The surface rms roughness obtained by atomic force microscopy (AFM) measurements increased with increasing LSMO channel thickness from 0.2 nm (layer-by-layer growth; see Fig. 2) for $d = 5$ nm to about 10 nm (due to a pronounced columnar growth) and was 0.9 nm for the 530 nm PZT film. X-ray photoelectron spectroscopy (XPS) analysis points towards SrO termination of the LSMO films at their free surface. The thicker LSMO films show Curie temperatures T_C around 345 K (70 nm) obtained from superconducting quantum interference device (SQUID) magnetometer measurements. The resistive transition is above 300 K for all devices, and the magnetoresistive properties are as usual for LSMO (see previous work[11] for details). The stoichiometry of the PZT thin films has been checked with XPS to be the same as that of the target within an accuracy of $\sim 5\%$. A typical ferroelectric polarization $P(E)$ loop of a device is plotted in Fig. 3. The saturation polarization is about 34 μC/cm^2, the remanent polarization is 30 μC/cm^2, and the coercive field $E_C = 47$ kV/cm (2.5 V) for a maximum voltage of 4 V.

Note that the $P(E)$ loop (if shifts along both axes are neglected) is antisymmetric in nature, i.e., it fulfills the relation $P(-E) = -P(E)$. In contrast, the piezoelectric strain of a PZT film is symmetric with respect to the sign of voltage (Fig. 4). (In real films, symmetry is disturbed, e.g., by substrate-induced strain of the PZT film and charge accumulations.) The minima appear near the coercive fields of electric polarization. Note that there is no saturation at larger voltages where the polarization is saturated.[12] This fundamentally different behavior can be used to distinguish the modulations from both field and strain effects.

The measured LSMO channel resistance modulated by an applied gate voltage is shown in Fig. 5. The hysteresis loops differ significantly for the four devices shown (5, 7, 45, and 70 nm channels). The 7 nm channel hysteresis loop [Fig. 5(a)] is butterflylike shaped with a total modulation of $\Delta R/R \sim 0.2\%$ ($R = 6.7$ kΩ). For both positive and negative voltages the channel resistance increases, even at maximum voltages where the measured polarization of the contact is saturated. The center crossover and the minima near the coercive fields E_C are slightly shifted towards positive voltages by 1 V. The sample with 5 nm channel thickness shows a similar butterfly loop [Fig. 5(a), inset]. By comparison with the inverse piezoeffect plotted in Fig. 4, we identify the butterflylike resistance loops as straininduced. The resistance changes nearly linearly with the gate voltage until the polarization switches at the respective coercive field. This is a characteristic of epitaxial films with (001) orientation where

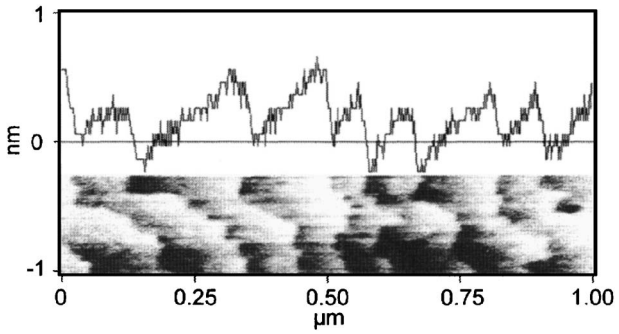

FIG. 2. AFM (tapping mode) line scan and topograph of the 5 nm LSMO channel surface showing single-layer steps of ~ 4 Å height.

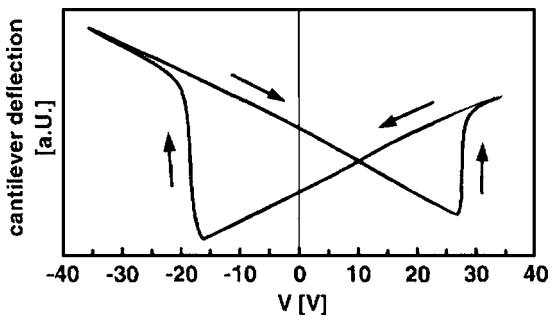

FIG. 4. Tip deflection of a cantilever covered with a 2.9-μm-thick (001)-oriented PZT film which is proportional to the in-plane strain of the film. Data reproduced from Kanno *et al.* (Ref. 12).

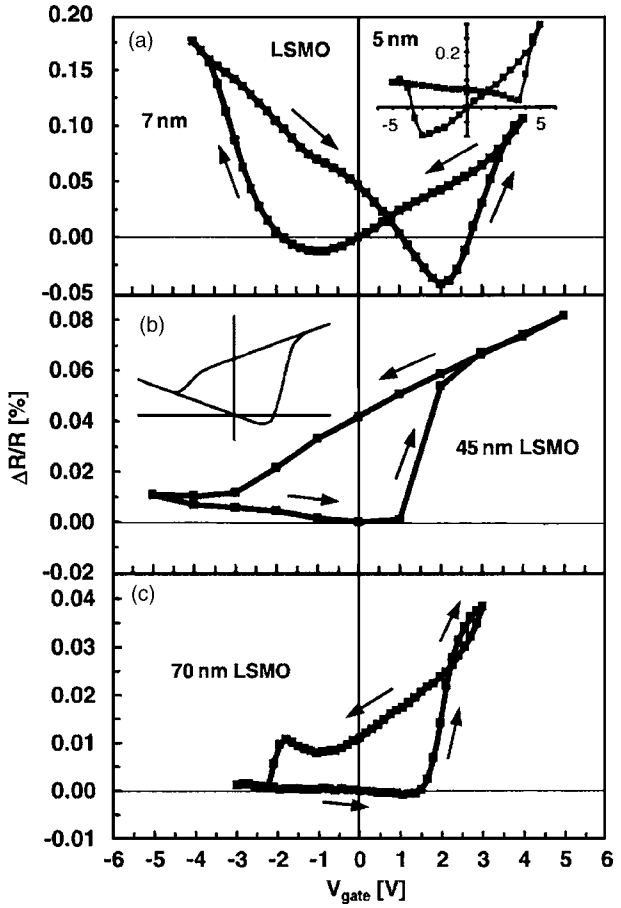

FIG. 5. Resistance hysteresis vs gate voltage at 300 K of devices (Fig. 1) with LSMO channel thickness as indicated. $\Delta R/R=[R(V_{\text{gate}})-R(0)]/R(0)$, $R(0)$ denotes the lower value of remanent resistance. The inset in (b) shows a calculated resistance loop for a combination of field effect and piezoelectric strain effect.

domain switching by 180° takes place. The value of $\Delta R/R$ is small because the films are clamped to the substrate. The strain underlying this resistance modulation can be roughly estimated considering the resistance changes observed in the LSMO films (of same stoichiometry and 50 nm thickness) on piezoelectric substrates. Lee *et al.* obtained $\Delta R/R=12\%$ at 290 K for $\Delta a=0.2\%$ of averaged biaxial in-plane strain on $BaTiO_3$.[13] In a recent experiment,[14] we found $\Delta R/R=9\%$ for $\Delta a=0.06\%$ at 300 K. Thus, the ratio between relative resistance and strain variations is approximately 100 for 50 nm LSMO films, allowing very sensitive strain detection. According to this estimation, the average in-plane strain in our FETs should be of the order of $10^{-3}\%$ only.

The hysteresis loop of the 70 nm channel [Fig. 5(c)] exhibits some features of a square-shaped hysteresis loop being characteristic of the electric field effect.[7] For positive (negative) voltages the resistance is larger (smaller) as expected for the field effect in an underdoped manganite where a positive electric field causes depletion of the holelike charge carriers. The 45 nm channel hysteresis loop in Fig. 5(b) resembles the curve in (c) but does not show saturation at large V_{gate}. A weighted addition of a butterflylike loop and a square-shaped loop gives the simulated curve presented in the inset which fairly well resembles the measured curve. It seems reasonable to assume a superposition of strain effect and field effect for this type of FET structure. Both can be approximately separated in a way attributing the resistance difference in the saturated state to field effect and the difference of slopes dR/dV_{gate} at $V_{\text{gate}}=0$ to strain modulation.

It is useful to note that the observation of strain-induced resistance modulation in the present FET devices was possible because the field effect in the $La_{0.7}Sr_{0.3}MnO_3$ channels was very low. This can be understood considering the bulk phase diagram[15] of $La_{1-x}Sr_xMnO_3$. The $x=0.3$ doping is on the plateau of optimum doping with maximum T_C. Hence, small variation of charge density should have little effect on magnetism and electrical resistance. Indeed, thin films may have a modified phase diagram due to the influence of substrate-induced strain. Furthermore, the interface terminations on both sides of the LSMO layer may provide an extra charge density or conducting interface states.[16] However, none of these phenomena seems to drive the behavior of the investigated LSMO channels far away from what is expected according to the bulk phase diagram.

Here, the magnitude of strain-induced $\Delta R/R$ decreases with increasing channel thickness. However, it is unclear if an equal strain level is achieved in all devices. The roughness of LSMO-PZT interface increases essentially with the LSMO thickness, and mechanical coupling of the heteroepitaxial components in dependence on roughness is unknown. On the other hand, magnetic/electric response to biaxial strain of a manganite film may depend on its thickness. Possibly, the ultrathin films (<10 nm) are particularly sensitive to lattice distortion. More work on the effect of controlled biaxial strain in films on piezoelectric substrates is underway.[14]

The authors gratefully acknowledge financial support by the Deutsche Forschungsgemeinschaft, Forschergruppe 520 and discussions with G. Suchaneck and L. Eng.

[1] S. Mathews, R. Ramesh, T. Venkatesan, and J. Benedetto, Science **276**, 238 (1997).
[2] H. Ota, H. Fujino, S. Migita, S.-B. Xiong, and S. Sakai, J. Appl. Phys. **89**, 8153 (2001).
[3] D. Marré, A. Tumino, E. Bellingeri, I. Pallecchi, L. Pellegrino, and A. S. Siri, J. Phys. D **36**, 896 (2003).
[4] H. Tabata and T. Kawai, IEICE Trans. Electron. **E80-C**, 918 (1997).
[5] S. B. Ogale, V. Talyansky, C. H. Chen, R. Ramesh, R. L. Greene, and T. Venkatesan, Phys. Rev. Lett. **77**, 1159 (1996).
[6] X. Hong, A. Posadas, A. Lin, and C. H. Ahn, Phys. Rev. B **68**, 134415 (2003).
[7] T. Kanki, Y.-G. Park, H. Tanaka, and T. Kawai, Appl. Phys. Lett. **83**, 4860 (2003).
[8] T. Zhao, S. B. Ogale, S. R. Shinde, and R. Ramesh, Appl. Phys. Lett. **84**, 750 (2004).
[9] D. Dale, A. Fleet, J. D. Brock, and Y. Suzuki, Appl. Phys. Lett. **82**, 3725 (2003).
[10] B. Holzapfel, B. Roas, L. Schultz, P. Bauer, and G. Saemann-Ischenko, Appl. Phys. Lett. **61**, 3178 (1992).
[11] C. Thiele, K. Dörr, W.-M. Lin, K.-H. Müller, and L. Schultz, Sens. Actuators, A (in press).
[12] I. Kanno, H. Kotera, and K. Wasa, Sens. Actuators, A **107**, 68 (2003).
[13] M. K. Lee, T. K. Nath, C. B. Eom, M. C. Smoak, and F. Tsui, Appl. Phys. Lett. **77**, 3547 (2000).
[14] C. Thiele, K. Dorr, L. Schultz, D. C. Meyer, A. A. Levin, and P. Paufler, Appl. Phys. Lett. (submitted).
[15] A. Urushibara, J. Morimoto, T. Arima, A. Asamitsu, G. Kido, and J. Tokura, Phys. Rev. B **51**, 14103 (1995).
[16] A. Ohtomo and H. Y. Hwang, Nature (London) **427**, 423 (2004).